International Journal of Thermophysics, Vol. 28, No. 1, February 2007 (© 2006)
DOI: 10.1007/s10765-006-0134-2

Uncertainty Analysis of Thermophysical Property Measurements of Solids Using Dynamic Methods

Svetozár Malinarič

Received December 22, 2005

This work reports on an analysis of thermophysical properties (thermal conductivity, thermal diffusivity, and specific heat capacity) measurements of solids using dynamic methods. The influence of temperature measurement uncertainty on the parameter estimation uncertainty is studied using a least-squares procedure. The standard and difference analyses are used for optimizing the experiment with respect to the data window or time interval of measurements. The analysis is applied to the extended dynamic plane source method, and the results of numerical computations are illustrated in the form of contour plots.

KEY WORDS: difference analysis; least-squares fitting; specific heat capacity; standard analysis; thermal conductivity; thermal diffusivity; transient method; uncertainty.

1. INTRODUCTION

Dynamic methods [1] for measuring thermophysical properties of solids (thermal conductivity, thermal diffusivity, and specific heat) represent a large group of techniques that use a dynamic temperature field inside the specimen. Dynamic methods can be characterized as follows. The temperature of the specimen is stabilized and uniform. Then a dynamic heat flow in the form of a pulse or step-wise function is applied to the specimen. The above mentioned thermophysical properties can be calculated from the temperature response.

The theoretical model of the experiment is established using a partial differential equation for the heat transport. The temperature function is a

Department of Physics, Constantine the Philosopher University, Trieda Andreja Hlinku 1, SK-949 74 Nitra, Slovakia. E-mail: smalinaric@ukf.sk

solution of this equation with boundary and initial conditions defined by a model which corresponds to the experimental arrangement. The experiment consists of measuring the temperature response and fitting the temperature function over the interval of experimental points.

The reliability of every measurement result is confirmed by a quantitative assessment of its uncertainty [2]. The sources of uncertainty in dynamic methods can be divided into two groups. The first group represents uncertainties caused by deviations of the mathematical model from the experimental setup. The second group comprises uncertainties of input parameter measurements and the evaluation method.

The objective of this work is to analyze the influence of the temperature measurement uncertainty on the thermophysical properties uncertainty. All other uncertainty components will be considered to be negligible. The analysis will be applied to the extended dynamic plane source (EDPS) method [3].

2. UNCERTAINTY ASSESSMENT IN LEAST-SQUARES PROCEDURE

The first step of evaluation is to determine the temperature function—temperature increase as a function of time t. Assume the function is of a known analytical form,

$$T(t, \vec{\alpha}) = T(t, \alpha_1, \alpha_2, \ldots \alpha_p) \tag{1}$$

where $\vec{\alpha}$ is a vector of unknown parameters [4]. In addition to the thermophysical parameters, there are usually some perturbation parameters [5] connected with the model. In this analysis, we assume that the deviation between model and experiment is negligible and the only source of uncertainty stems from the temperature measuring uncertainty. We also assume that the uncertainties of temperature measurement of all points are the same and the uncertainty of the time measurement is negligible. Since the temperature function, Eq. (1), is nonlinear in the parameters, we expand it using a Taylor series [6]. Then we can write the linear least-squares procedure in matrix notation;

$$\vec{Y} - \vec{T}_0 = \mathrm{X} \cdot (\vec{\alpha} - \vec{a}) + \vec{\varepsilon} \tag{2}$$

where $\vec{Y}$ is the observation vector of temperature measured at n points t_i and $\vec{a}$ represents an educated guess for the parameter vector $\vec{\alpha}$, which can be determined using standard nonlinear least-squares fitting [4]. $\vec{\varepsilon}$ is the

vector of errors and $\vec{T}_0$ is the vector of temperatures given by the temperature function, Eq. (1), as follows:

$$\left\{\vec{T}_0\right\}_i = T\left(t_i, \vec{a}\right). \tag{3}$$

X is the sensitivity matrix [4] that is given by

$$\{\mathbf{X}\}_{ij} = \beta_j\left(t_i, \vec{\alpha}\right) \tag{4}$$

where β_j is the sensitivity coefficient for parameter α_j defined by

$$\beta_j\left(t, \vec{\alpha}\right) = \frac{\partial T(t, \vec{\alpha})}{\partial \alpha_j}. \tag{5}$$

The standard uncertainty of the least-squares estimate of the parameter α_j is

$$u^2\left(\alpha_j\right) = \{\mathbf{M}\}_{jj}\, u^2(T) = \left(A_j\, u(T)\right)^2 \tag{6}$$

where $u(T)$ is the standard uncertainty of temperature measurement and the matrix **M** is given by

$$\mathbf{M} = \left(\mathbf{X}^T \cdot \mathbf{X}\right)^{-1}. \tag{7}$$

According to Eq. (6), the uncertainty of the parameter estimate $u\left(\alpha_j\right)$ consists of two components. The first component, designated as coefficient A_j, is given by the temperature function and selection of values t_i in Eq. (4). The second component is given by the temperature measurement uncertainty. The parameter estimates are correlated because they stem from the same reading points. The degree of correlation between estimates of parameter α_i and α_j is characterized by the correlation coefficient defined by

$$r_{ij} = \frac{\{\mathbf{M}\}_{ij}}{\sqrt{\{\mathbf{M}\}_{ii}\{\mathbf{M}\}_{jj}}} \tag{8}$$

3. STANDARD AND DIFFERENCE ANALYSIS

In this section, we focus on optimizing the experiment with respect to a data window defined by the time interval$(t_B, t_B + t_S)$, where t_B is the time at the beginning of the time interval and t_S is the size of the interval, as shown in Fig. 1. The standard and difference analyses [7] are methods of determining an optimal time interval, in which the fitting procedure gives results with minimum values of measurement error. The standard analysis is based on estimating parameters using a least-squares procedure when t_B is constant while t_S is successively increased. The results of fitting are plotted against t_S. In the difference analysis, on the contrary, t_B is the variable and t_S is the constant. The results of fitting are plotted against t_B. The principle of the analyses consists of the assumption that the time interval $(t_B, t_B + t_S)$ is optimal when the results of fitting are not sensitive to changes of this interval, which causes the plots to have a plateau.

Both methods can be applied to data from real measurements where all types of uncertainties are included. They can also be used in experiment modeling where the only source of uncertainty is simulated, e. g., as random noise of the temperature measurement. The third application is a plot of the time dependence of coefficient A_j. As can be seen from Eq. (6), a low value of A_j predicts a low value of parameter uncertainty $u(\alpha_j)$ and, thus, a low value of measurement error.

4. DIMENSIONLESS QUANTITIES

Dimensionless quantities [8] enable one to perform universal numerical calculations with arbitrary specimen dimensions and thermophysical

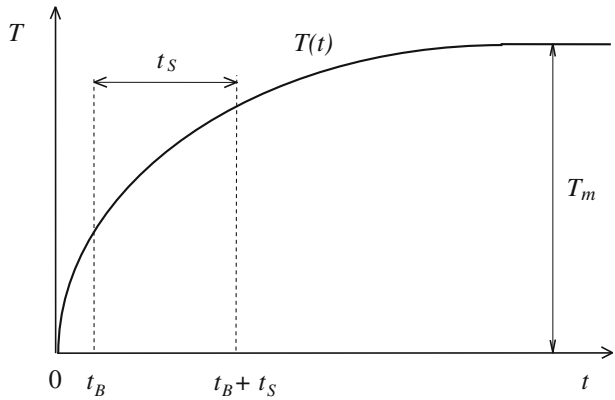

Fig. 1. Temperature function and data window definition.

properties. The dimensionless time is defined by

$$t^+ = \frac{a \cdot t}{l} \tag{9}$$

where a is the thermal diffusivity and l is a characteristic dimension of the specimen. The dimensionless temperature is defined by the following form:

$$T^+ = \frac{T}{T_\mathrm{m}} \tag{10}$$

where T_m is the maximum value of temperature reached between the start and end of the experiment. Similarly, we can define dimensionless sensitivity coefficients,

$$\beta_j^+ (t, \vec{\alpha}) = \frac{\alpha_j}{T_\mathrm{m}} \frac{\partial T(t, \vec{\alpha})}{\partial \alpha_j}. \tag{11}$$

and also dimensionless coefficients A_j^+ according to Eq. (6),

$$u^+ (\alpha_\mathrm{j}) = \frac{u(\alpha_j)}{\alpha_j} = \frac{A_j \cdot T_\mathrm{m}}{\alpha_j} \cdot \frac{u(T)}{T_\mathrm{m}} = A_j^+ \cdot u^+ (T) \tag{12}$$

where u^+ is a dimensionless (≡relative standard) uncertainty [2].

5. EXTENDED DYNAMIC PLANE SOURCE METHOD

The extended dynamic plane source method is characterized by stepwise heating and one-dimensional heat flow into a finite specimen [3]. The experimental arrangement is depicted in Fig. 2. The heat is produced by the passage of an electrical current through a nickel-disc sensor, which simultaneously serves as the thermometer. Two identical specimens

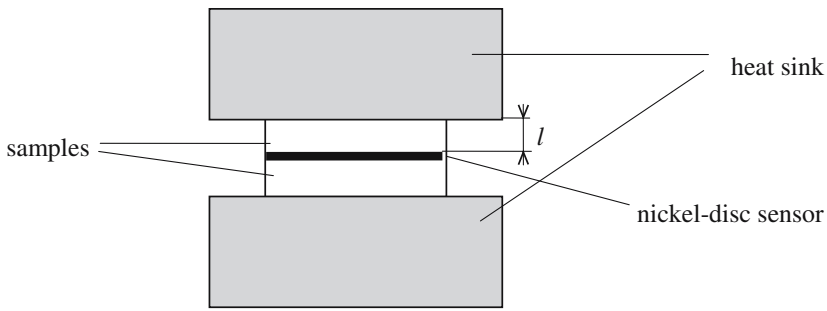

Fig. 2. Setup of the experiment.

of cylindrical shape cause symmetrical division of heat flow into very good heat conducting materials (heat sink) to provide isothermal boundary conditions for the experiment. The disc temperature is determined by measuring its electrical resistance. The temperature function is given by

$$T(t, a, \lambda, \tau) = \frac{q}{\lambda}\sqrt{\frac{ta}{\pi}}\left(1 + 2\sqrt{\pi}\sum_{n=1}^{\infty} B^n \text{ierfc}\left(\frac{nl}{\sqrt{at}}\right)\right) + \tau \tag{13}$$

where q is the heat flow rate supplied per unit area of the specimen, l is the thickness, λ is the thermal conductivity, and a is the thermal diffusivity of the specimen. The perturbation parameter τ is the offset referred to the additional increase in temperature of the disc due to its imperfections (heat capacity of the disc and thermal contact between disc and specimen). B describes the heat sink imperfection determined by its effusivity [3] and ierfc is the error function integral [9]. Both thermophysical properties λ and a can be estimated by fitting the temperature function to the experimental points. Their uncertainties are given by Eq. (6). The maximum value of the temperature function is given by

$$T_{\text{m}} = \frac{q \cdot l}{2 \cdot \lambda} \tag{14}$$

The third thermophysical property—specific heat capacity c—can be determined from

$$c = f(a, \lambda, \rho) = \frac{\lambda}{a\,\rho} \tag{15}$$

where ρ is the specimen density. Here a, λ, and ρ represent input quantities upon which the output quantity c depends through a functional relationship f. Since the input estimates of a and λ were determined by a least-squares procedure, they should be regarded as correlated. The combined variance of the parameter c is given by [2]

$$u^2(c) = \left(\frac{\partial f}{\partial a}\right)^2 u^2(a) + \left(\frac{\partial f}{\partial \lambda}\right)^2 u^2(\lambda) + 2\left(\frac{\partial f}{\partial a}\right)\left(\frac{\partial f}{\partial \lambda}\right) u(a, \lambda) \tag{16}$$

where $u(a, \lambda)$ is the estimated covariance associated with a and λ. Introducing dimensionless quantities and using Eqs. (15), (16), and (12), we obtain

$$\left(A_c^+\right)^2 = \left(A_a^+\right)^2 + \left(A_\lambda^+\right)^2 - 2A_a^+ A_\lambda^+ r(a, \lambda) \tag{17}$$

where $r(a, \lambda)$ is the correlation coefficient associated with a and λ defined by Eq. (8).

6. RESULTS AND DISCUSSION

Figure 3 shows the temperature and two sensitivity coefficients as a function of time on a dimensionless scale. A sensitivity coefficient is a measure of the change in temperature function with an estimated parameter. The sensitivity coefficients analysis is based on the assumption that the fitting procedure does not work properly when sensitivity coefficients are small or linearly dependent on each other [4]. But it is difficult to determine the optimal time interval directly from Fig. 3. Some methods for quantification of the linear dependence of the sensitivity coefficients have been elaborated. In Ref. 10, the linear dependence was quantified using local curvature of the line when one sensitivity coefficient is plotted against the other. In Ref. 11, the linear dependence was investigated by the use of the Wronskian. In both papers, the optimal time interval was determined when the sensitivity coefficients were not linearly dependent. But there was no evidence of a minimum of measurement error in this interval.

This problem will be solved by means of computing the parameter estimate uncertainty for all possible time intervals using Eq. (12). This represents an integration of the standard and difference analysis described in Section 3. Since the temperature measurement uncertainty $u(T)$ is assumed to be constant, it proves to be useful to investigate only the

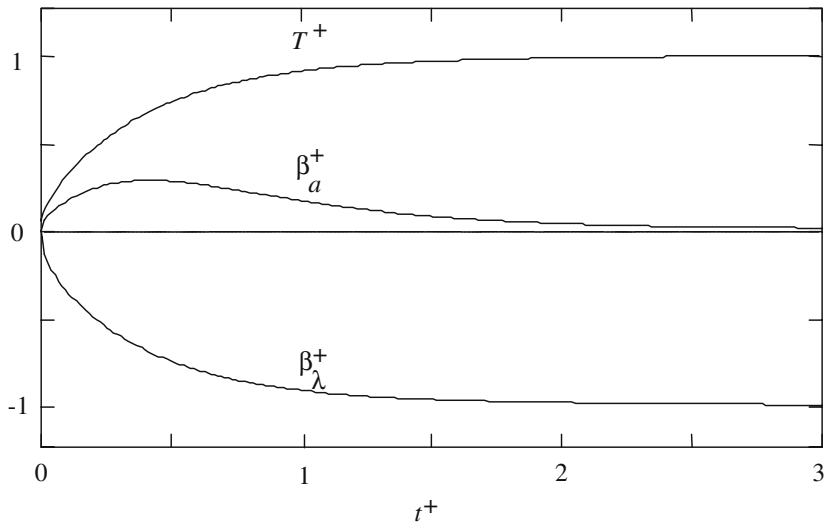

Fig. 3. Dimensionless temperature function and dimensionless sensitivity coefficients β_a^+ and β_λ^+ versus dimensionless time in EDPS method.

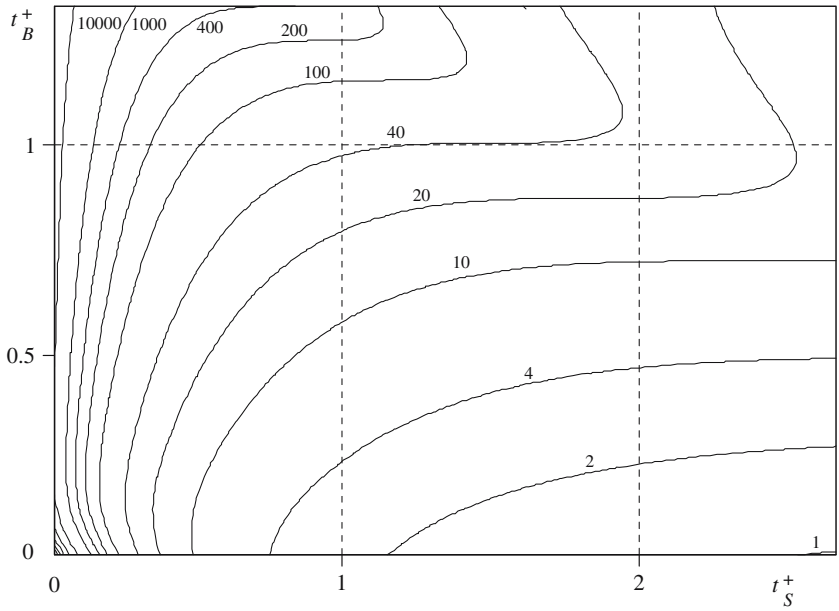

Fig. 4. Contour plot of dimensionless coefficient A_a^+ as a function of dimensionless times t_S^+ and t_B^+.

coefficients A_a^+, A_λ^+, and A_c^+ associated with the corresponding thermophysical properties. Figure 4 shows the dimensionless coefficient A_a^+ as a function of two variables t_s^+ and t_B^+ in the form of a contour plot which can be used to determine directly the expected uncertainty of parameter estimation for a given time interval. To simplify the construction of the contour plot, the sampling period was set to 1 s so that the following values were used in Eq. (4) $t_1 = t_B$, $t_2 = t_B + 1\,\mathrm{s} \ldots t_n = t_B + t_S$. The plot was created using Mathcad software and formatted to logarithmic scale. In Fig. 4, we see that there is no local minimum and the coefficient is decreasing with the size of the interval. Similarly, Fig. 5 shows the contour plot of the dimensionless coefficient A_λ^+. The contour lines show the "valley" along the straight line p with points A, B, and C. This is the region where low values of uncertainty can be expected.

Figure 6 shows the correlation coefficient $r(a, \lambda)$ as a function of two variables t_s^+ and t_B^+ in the form of a contour plot. Comparing Figs. 5 and 6, we notice that the correlation coefficient changes sign just along the straight line p.

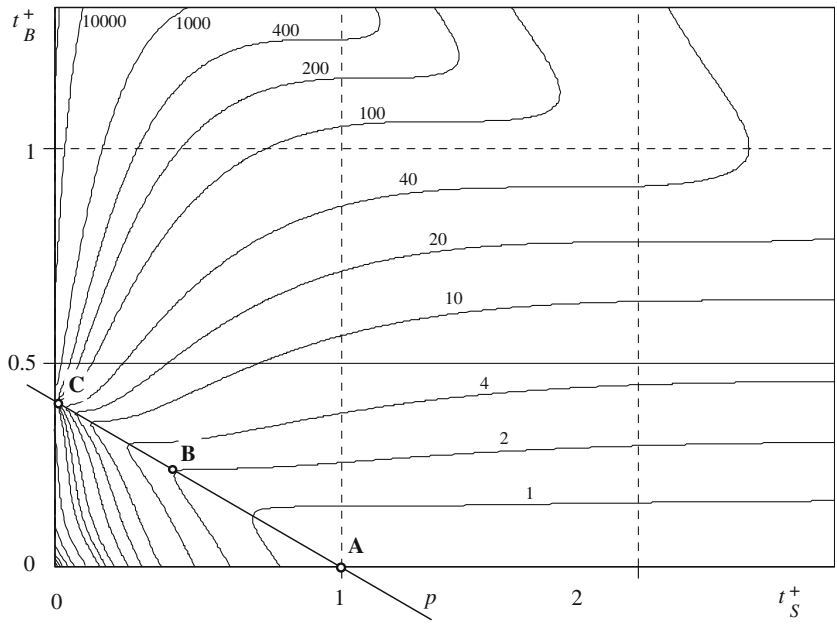

Fig. 5. Contour plot of dimensionless coefficient A_λ^+ as a function of dimensionless times t_S^+ and t_B^+.

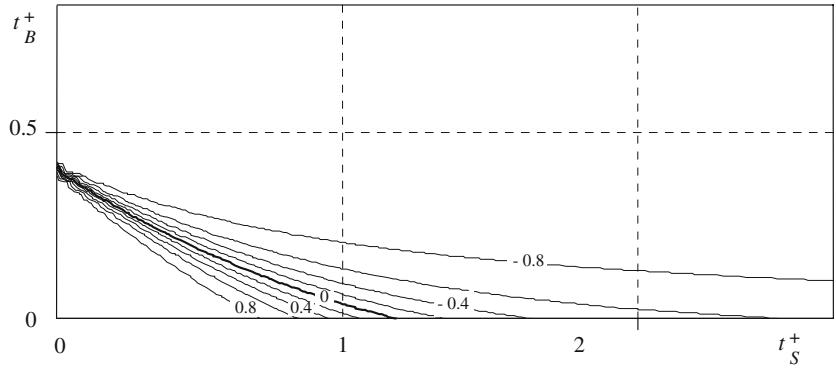

Fig. 6. Contour plot of correlation coefficient $r(a, \lambda)$ as a function of dimensionless times t_S^+ and t_B^+.

Table I. Uncertainty Evaluation for Time Intervals Defined by Points A, B, and C in Fig. 5.

Point	t_B^+	t_S^+	Time interval (s)	A_a^+	A_λ^+	$r(a,\lambda)$	A_c^+	$u^+(a)$ (%)	$u^+(\lambda)$ (%)	$u^+(c)$ (%)
A	0	1	(0; 75)	2.3	0.61	0.53	2.0	0.62	0.16	0.54
B	0.24	0.4	(18; 48)	18	2.1	0	18	4.9	0.57	4.9
C	0.4	0.03	(30; 32)	8400	94	0.63	8300	2300	26	2200

Figures 7, 8, and 9 show the dependences of dimensionless coefficients A_a^+, A_λ^+, A_c^+ and the correlation coefficient $r(a,\lambda)$ with dimensionless time t_B^+ for three values of t_S^+ (1, 0.4, and 0). These plots represent the results of difference analyses described in Section 3. Points A, B, and C are situated at minima of curves and were selected for the uncertainty evaluation in Table I.

The analysis was tested simulating measurements of PMMA (polymethylmetacrylate). The following values were used: $l = 0.003\,\mathrm{m}$, $q = 500\,\mathrm{W{\cdot}m^{-2}}$, $a = 0.12 \times 10^{-6}\,\mathrm{m^2{\cdot}s^{-1}}$, $\lambda = 0.19\,\mathrm{W{\cdot}m^{-1}{\cdot}K^{-1}}$, $\tau = 0.2\,\mathrm{K}$, and $B = -0.954$. The sampling period was 1 s and the standard uncertainty of temperature measurement $u(T) = 0.01\,\mathrm{K}$. Table I shows the uncertainty evaluation for three different time intervals. Using Eq. (9), the dimensionless time was retransformed into real time. The dimensionless coefficients were determined from Figs. 7 to 9. The relative standard uncertainties of thermophysical properties estimates were obtained by using Eqs. (12) and (17).

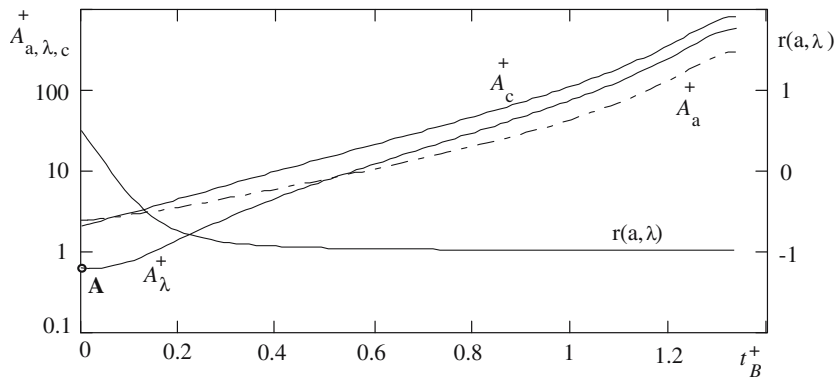

Fig. 7. Values of dimensionless coefficients A_a^+, A_λ^+, A_c^+ and correlation coefficient $r(a,\lambda)$ versus dimensionless time $t_B^+(t_S^+ = 1)$.

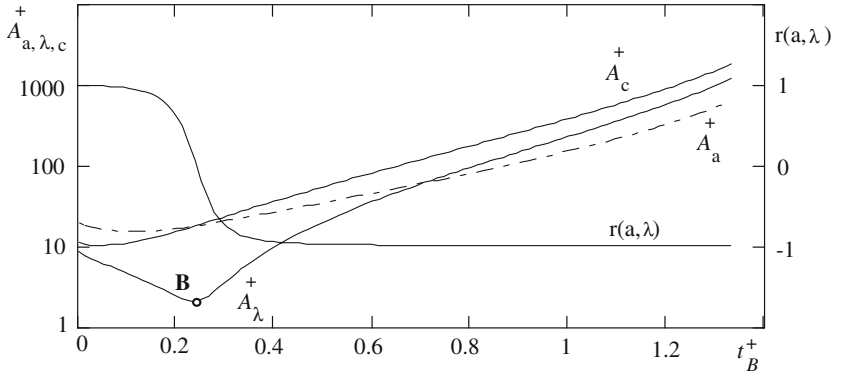

Fig. 8. Values of dimensionless coefficients A_a^+, A_λ^+, A_c^+ and correlation coefficient $r\,(a, \lambda)$ versus dimensionless time $t_B^+ (t_S^+ = 0.4)$.

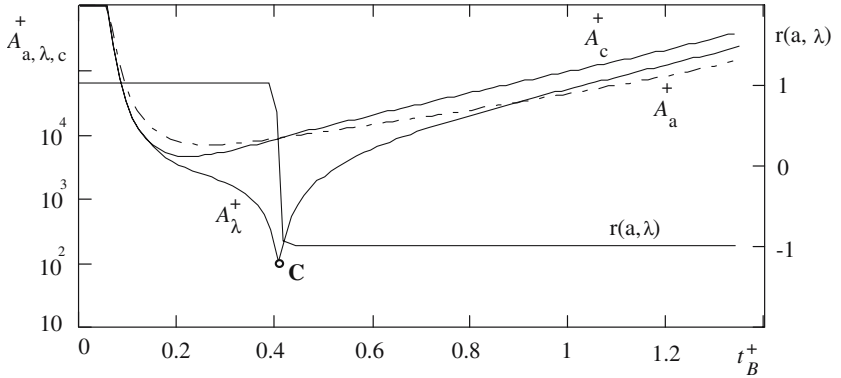

Fig. 9. Values of dimensionless coefficients A_a^+, A_λ^+, A_c^+ and correlation coefficient $r\,(a, \lambda)$ versus dimensionless time $t_B^+ (t_S^+ = 0.03)$.

The sharp minimum in Fig. 9 predicts that the optimal time interval would have a non-zero beginning, because the optimization consists of finding the time interval that gives the minimal value of measurement uncertainty. This is in agreement with the results published in Refs. 10–12 where the time interval was determined approximately as $t_B^+ = 0.1$ and $t_S^+ = 1$. But current analysis shows that the curves in Fig. 7 acquire their minima at $t_S^+ = 1$ and $t_B^+ = 0$ (point A). Hence, from a theoretical point of view, there is no reason for omitting data at the beginning of the time series.

The results of the presented analysis were compared with those from experiment [10], where the following deviations between the experiment and the theoretical model were demonstrated. At the beginning of the

measurement, a deviation is caused by the imperfection of the disc, and at the end, by heat losses from the sample. The fitting procedure was applied in the window from 10 to 80 s, where deviations were negligible. The main source of uncertainty in the EDPS method was measurement repeatability caused probably by inaccurate positioning of the disc and specimens in the holder. The combined standard uncertainty was evaluated at 3.6% for the thermal conductivity and 2.7% for the thermal diffusivity. These values are considerably higher than that in Table I for point A, which are results for the only source of uncertainty-temperature measurement.

The temperature measurement uncertainty $u(T)$ in Eq. (6) is supposed to be caused by random noise and does not include any systematic error. The value of 0.01 K has been taken from the plot of residuals in Fig. 11 [10]. The systematic error in temperature measurement is corrected using the perturbation parameter τ in Eq. (13).

7. CONCLUSIONS

The paper presents an analysis of the influence of temperature measurement uncertainty on the uncertainty of the least-squares estimate of the thermophysical properties. The analysis is based on numerical computation of the parameter estimate uncertainty for all possible time intervals. The coefficients of uncertainty A_a^+, A_λ^+, and A_c^+ and the correlation coefficient $r(a, \lambda)$ are plotted as functions of two variables t_S^+ and t_B^+ (Figs. 4–9). The analysis is applied to the thermophysical properties measurement of PMMA by using the EDPS method (Table I). The analysis shows that at shorter intervals ($t_S^+ = 0.4$), the minimum uncertainty is obtained at a non-zero interval beginning time (Fig. 8, point B), but at longer intervals ($t_S^+ = 1$) the minimum is at $t_B^+ = 0$ (Fig. 7, point A). The main contribution of this work consists of introducing the coefficient of uncertainty in Eq. (6) and its application in the standard and difference analysis and uncertainty minimalization.

ACKNOWLEDGMENT

Author wishes to thank the Slovak Science Grant Agency for financial support under Contract 1/3178/06.

REFERENCES

1. L'. Kubičár and V. Boháč, *Proc. 24th Int. Conf. on Thermal Conductivity/12th Int. Thermal Expansion Symp.*, P. S. Gaal and D. E. Apostolescu, eds. (Technomic, Lancaster, Pennsylvania, 1999), p. 135

2. *Guide to the Expression of the Uncertainty in Measurement* (ISO, Geneva, 1993).
3. E. Karawacki, B. M. Suleiman, I. ul-Haq, and B. Nhi, *Rev. Sci. Instrum.* **63**:4390 (1992).
4. J. V. Beck and K. J. Arnold, *Parameter Estimation in Engineering and Science* (Wiley, New York, 1977).
5. L. Vozár and G. Groboth, *High Temp.-High Press.* **29**:191 (1997).
6. F. Kundracik, *Spracovanie experimentálnych dát* (UK, Bratislava, 1999).
7. V. Boháč, M. K. Gustavsson, L'. Kubičár, and S. E. Gustafsson, *Rev. Sci. Instrum.* **71**:2452 (2000).
8. R. Taktak, J. V. Beck, and E. P. Scott, *Int. J. Heat Mass Transf*er **36**:2977 (1993).
9. H. S. Carslaw and J. C. Jaeger, *Conduction of Heat in Solids* (Clarendon, Oxford, 1959).
10. S. Malinarič, *Meas. Sci. Technol.* **15**:807 (2004).
11. S. Malinarič, *Int. J. Thermophys.* **25**:1913 (2004).
12. S. Malinarič and P. Ďuríšek, *Acta Phys. Slovaca* **55**:165 (2005).